Journal of Molecular Structure 1148 (2017) 238–246

Contents lists available at ScienceDirect

Journal of Molecular Structure

journal homepage: http://www.elsevier.com/locate/molstruc

Synthesis, X-ray crystal structures, electrochemistry and theoretical investigation of a tetradentate nickel and copper Schiff base complexes

Samra Rahmouni [a], Amel Djedouani [b, c], Barkahem Anak [c, d], Salima Tabti [e], Abderrahmen Bendaas [a], Mustapha Bencharif [c, d], Michel François [f], Solenne Fleutot [f], Franck Rabilloud [g, *]

[a] Laboratoire d'Electrochimie des Matériaux Moléculaires et Complexes (LEMMC), Département de Génie des procédés, Faculté de Technologie, Université Ferhat Abbas Sétif-1, Algeria
[b] Laboratoire de Physicochimie Analytique et Cristallochimie des Matériaux Organométalliques et Biomoléculaires, Constantine1, Algeria
[c] Ecole normale supérieure de Constantine, Ville Universitaire Ali Mendjli, Constantine 3, Algeria
[d] Laboratoire de chimie des matériaux de Constantine, Faculté des Sciences Exactes, Université des frères Mentouri-Constantine, 25000, Algeria
[e] Faculté des sciences et technologie, département SM, Université de Mohamed el Bachir el Ibrahimi, El Anasser, Bordj Bou-Arréridj, 34000, Algeria
[f] Institut Jean Lamour UMR 7198, Parc de Saurupt, CS 14234, F 54042, Nancy, France
[g] Univ Lyon, Université Claude Bernard Lyon 1, CNRS, Institut Lumière Matière, F-69622, Villeurbanne, France

ARTICLE INFO

Article history:
Received 30 June 2017
Accepted 14 July 2017
Available online 15 July 2017

Keywords:
Metal complexes
Crystallography electrochemistry
Quantum chemical calculations (DFT)

ABSTRACT

New tetradentate mononuclear nickel(II) [NiL] and pentadentate binuclear copper(II) **[$Cu_2L_2H_2O$], H_2O** Schiff base complexes have been synthesized. The crystal structures of [NiL] and **[$Cu_2L_2H_2O$], H_2O** have been determined by X-ray diffraction method showing distorted square-planar geometry for [NiL] and distorted tetragonal pyramid geometry for **[$Cu_2L_2H_2O$], H_2O**. In both complexes, the dehydroacetic acid functional group engages in a deprotonated manner and coordination occurs through the nitrogen atoms of the imine function and the phenolic oxygen. Density Functional Theory calculations are carried out for the determination of the optimized structures. The fundamental vibrational wave numbers are calculated and a good agreement between observed and calculated wave numbers is achieved.

1. Introduction

Schiff base ligands that containing oxygen and nitrogen donors set represent one of the most widely utilized classes of ligands and have been of research interest in different aspects in recent decades, because of the versatility of their steric and electronic properties, which can be modified by choosing the appropriate amine precursors and ring substituents. Metal complexes with Schiff bases as ligands have played a considerable attention in the development of coordination chemistry because they have high stability and important properties in different oxidation states [1–4]. Some complexes with tetradentate N_2O_2 donor Schiff base ligands have been extensively studied in the past years [5,6]. Therefore, Schiff base ligands derived from dehydroacetic acid (dha = 3-acetyl-4-hydroxy-6-methyl-2H-pyrone-2-one) are widely used to coordinate various metal ions because of the high stability of their complexes [5–8]. Furthermore, studies have shown that such compounds and their complexes have very interesting biological activity such as antimicrobial, antifungal, antitumor and herbicides [9–17], pharmacological [18,19] and medicinal properties [20,21].

In this work, synthesis of [NiL] and **[$Cu_2L_2H_2O$], H_2O** complexes is reported using (N,N'-bis(dehydroaceto)ethylenediimine) as Ligand (L) (Scheme 1). Single crystal X-Ray Diffraction and quantum chemical calculations are used in order to confirm the structure of complexes. The spectral study using FT-IR, and UV–visible analyses are also investigated in order to find a correlation between molecular structure and vibrational frequencies of complexes. Electrochemical investigation of complexes is also performed.

* Corresponding author.
E-mail address: franck.rabilloud@univ-lyon1.fr (F. Rabilloud).

http://dx.doi.org/10.1016/j.molstruc.2017.07.032
0022-2860/

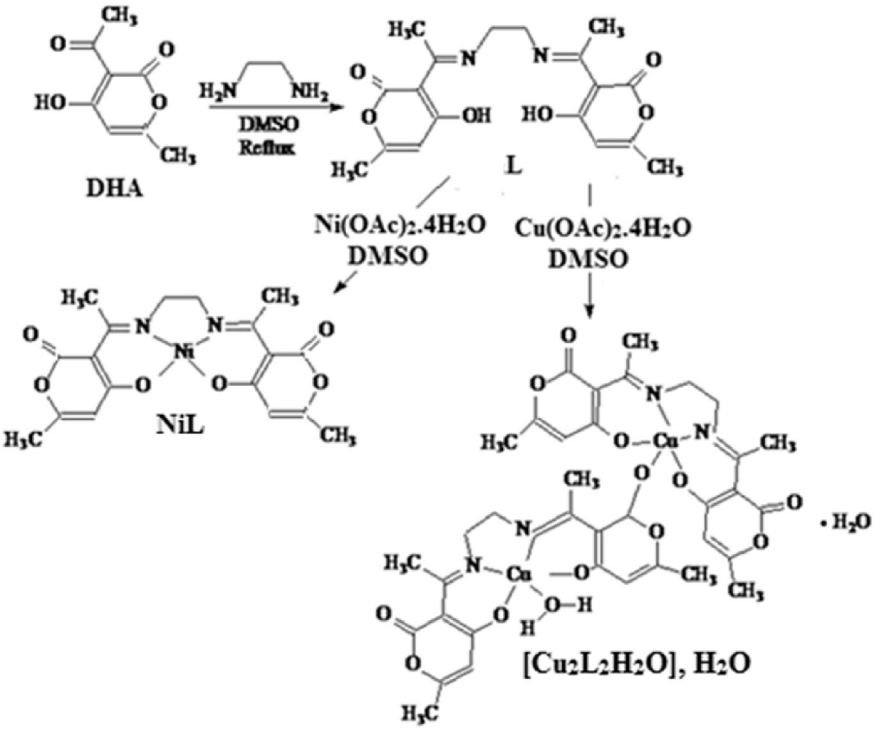

Scheme 1. Reaction way leading to the formation of the nickel and copper Schiff base complexes.

2. Experimental

2.1. Reactants

All reactants and solvents were analytical grade and used without further purification. Ethylendiamine and dehydroacetic acid was purchased from Sigma-Aldrich. Nickel and copper hydrated acetate (Prolabo) were used as received.

2.2. Measurements

The IR spectra were obtained on a Shimadzu FTIR-Affinity-1 spectrometer with KBr pellets in the 4000-400 cm^{-1} region. The electronic absorption spectra were carried out on a Shimadzu UV1800 spectrophotometer using DMSO as solvent. The melting point complexes were determined with a Kofler Banc 7779 apparatus. Cyclic voltammetry was performed with a VoltaMaster 4 software under a nitrogen atmosphere in a one-compartment electrolysis cell consisting of a glassy carbon working electrode (GC), a platinum wire counter electrode and all potentials are expressed versus the saturated solution of calomel electrode (SCE). Cyclic voltammograms were monitored at scan rates of 400, 300, 200, 100, 75, 50, 25 and 10 mV s^{-1} and recorded in DMSO. The concentrations of the complexes were maintained at 10^{-3} M, and each solution contained 0.1 M tetrabutylammonium perchlorate ($TBAPF_4$) as the electrolyte.

2.3. Crystal data collection and processing

X-ray single-crystal diffraction data were collected at 293 K on a Diffractomer Bruker-Nonius and goniometre Kappa CCD, equipped with a graphite monochromator using Mo/Ka radiation (λ = 0.71073 Å). Cell refinement and data reduction were carried out with the APEX2 Software [22]. Structures were solved by direct methods and refined on F^2 by full-matrix least-squares method, using SHELX97 package [23]. All non-H atoms were refined anisotropically by the full matrix least squares method on F^2 using SHELXL [24] and the H atoms were included at the calculated positions and constrained to ride on their parent atoms.

2.4. Computational studies

The geometry of complexes, in the gas phase, have been fully optimized within the density functional theory method (DFT) using the GAUSSIAN 09 program package [25], as DFT methods [26] are very effective in modeling compounds and have good experimental correlations with the IR frequencies. DFT calculations were performed using the hybrid Becke's three parameter and the Lee–Yang–Parr functional (B3LYP) [27,28], one of the most popular density functional method, and using 6-311G(d,p) and LANL2DZ basis sets.

2.5. Synthesis and characterization

2.5.1. Synthesis of the ligand (L)

The (N,N'-bis(dehydroaceto)ethylenediimine) ligand was prepared by the reaction of one mole of ethylendiamine with two mole of dehydroacetic acid in absolute EtOH according to the literature [29].

2.5.2. Synthesis of [NiL]

$Ni(OAc)_2.4H_2O$ (0.062 g, 0.25 mmol, 10 mL DMSO) was slowly added to the ligand (0.080 g, 0.25 mmol, 10 mL DMSO), under nitrogen atmosphere and refluxing conditions. The reflux was maintained for 25 h. By slow evaporation of the orange solution, single orange crystals of [NiL] were removed by filtration and then dried in vacuum. Yield: 65%; mp = 293 °C; FT-IR (KBr pellets, ν cm^{-1}): 3435 (O–H); 1560 (C=N); 1180 (C–O), 1643 (C=O); UV/Vis: DMSO, λ(nm) 281, 310, 370, 575.

2.5.3. Synthesis of [$Cu_2L_2H_2O$], H_2O

To a solution of ligand (0.25 mmol, 0.08 g, DMSO) was added $Cu(OAc)_2.4H_2O$ (0.062 g, 0.25 mmol, 10 mL DMSO) with a 1: 2 stiochiometric, under nitrogen atmosphere and refluxing conditions and kept at an appropriate temperature and then allowed to stand for two days. Single blue crystals of complex [$Cu_2L_2H_2O$], H_2O were removed by filtration and then dried in vacuum.

Yild: 75%; mp = 293 °C; IR (KBr pellets, ν cm^{-1}): 3421(O–H); 1378 (C–N); 1226 (C–O); 1691 (C=O); UV/Vis: DMSO, λ nm 260, 312, 374, 568.

3. Results and discussion

3.1. Infrared spectra

The infrared spectra of [NiL] and **[$Cu_2L_2H_2O$], H_2O** were analyzed in the region 4000–500 cm^{-1}. Fig. 1 shows a band at 3435 cm^{-1} assigned to intermolecular hydrogen bonded ν(OH) for [NiL] and band at 3421 cm^{-1} assigned to the OH vibration of aqua and coordinated water molecular for **[$Cu_2L_2H_2O$], H_2O**. The bands due to lactone carbonyl ν(C=O) and ν(C–O) were found at 1700 cm^{-1} and 1226 cm^{-1} (for [NiL] [30–32]) and 1691 cm^{-1} and 1226 cm^{-1} (for **[$Cu_2L_2H_2O$], H_2O** [33,34]). However, the absorption bands appearing at 1560 and 1378 cm^{-1} are assigned to the ν(C=N) stretching for both complexes respectively. Lower frequency region above 694 and 594 cm^{-1} in the spectra of [NiL] [15,35] and 625 and 567 cm^{-1} in the spectra of the [$Cu_2L_2H_2O$], H_2O were tentatively assigned to ν(M–N) and ν(M–O) vibrations.

3.2. Electronic absorption spectra

The formation of the metal complexes was also confirmed by UV–vis analysis since their electronic spectra, recorded as DMSO solution in the wavelength range 800–200 nm. For the [NiL] complex λ_{max} were observed at 281, 310, 370 and 575 nm assignable to $\pi \rightarrow \pi^*$, $n \rightarrow \pi^*$ and metal to ligand (MLCT) charge transfer transitions, respectively [36,37]. The last peak located at 575 nm obtained with a concentration of 10^{-3} M was ascribed to the d–d electronic transitions which are usually known by their weaker intensities [38].

[$Cu_2L_2H_2O$], H_2O complex gave four bands at λ_{max} at 260, 312, 374 and 568 nm assigned to $\pi \rightarrow \pi^*$, $n \rightarrow \pi^*$, metal to ligand (MLCT) charge transfer and d-d transitions. These results are in good agreement with the literature [39,40].

3.3. X-ray crystal structure

3.3.1. Crystal structure of [NiL]

The main crystal parameters are reported in Table 1. The structure of one structural unit and atoms numbering scheme are given in Fig. 2. The complex [NiL] is crystallized in a monoclinic system in $P2_1/c$ space group and with a four unit per cell (Z = 4). The complex has distorted square-planar geometry connected via two phenolic oxygen O_1 and O_4 and imine nitrogen N_1 and N_2 atoms in E configuration around the C_{17}–C_{18} bond, with an average of 92.92° in the six-membered metallocycle and 89.32° in the five membered metallocycle.

The two (dha) rings of the complex are not coplanar with the above coordination plane ($O_1N_2N_1O_4$) and make dihedral angle of 13.61°. The distances between the coordinated nitrogen and oxygen atoms and the metal center do not significantly differ (Table 2), and they are similar to the values found in the Ni^{II}–*N*,*N*′-bis(salicylaldehyde) ethylenediimine complex (Ni–O) = 1.83 Å,(Ni–N) = 1.86 Å [41], in the [NiL, H_2O] (Ni–O) = 1.833(4) Å, (Ni–N) = 1.856(4) Å [42]. The bond angles O_1–Ni–O_4, O_1–Ni–N_2, N_2–Ni–N_1, O_4–Ni–N_1 are 84.90(10), 93.17(11), 89.33(12) and 92.64(13) degrees respectively. The atoms N_1, N_2, O_1 and O_4 are coplanar and define the basal plane. The maximum of deviation is given by the oxygen atoms (0.027 Å).

In the crystal, individual molecules are packed in layers parallel, in which the molecules of the second layer are oriented in a nearly perpendicular fashion to each other (Fig. 3a), each two layers are linked by intermolecular hydrogen bonds between adjacent molecules (Fig. 3b).

*3.3.2. Crystal structure of **[$Cu_2L_2H_2O$], H_2O***

The main crystal parameters are reported in Table 1. The bond distances and angles are listed in Table 2 and the structure and the numbering scheme are given in Fig. 2. The complex [$Cu_2L_2H_2O$], H_2O crystallizes in a triclinic system with a P-1 space group and we note the presence of two molecules per unit cell. [$Cu_2L_2H_2O$], H_2O is binuclear, the structure reveals that the two Cu(II) center is "4 + 1" coordinated, exhibiting a highly distorted tetragonal pyramid geometry in which the basal plane is occupied by two oxygen atoms from the phenolates and two nitrogen atoms from the imine groups of the ligand, the axial position of Cu1 is occupied by O1w atom of water molecular and one pyrone oxygen from another moiety, in axial positions from Cu2. One Molecule of water links the two ligands.

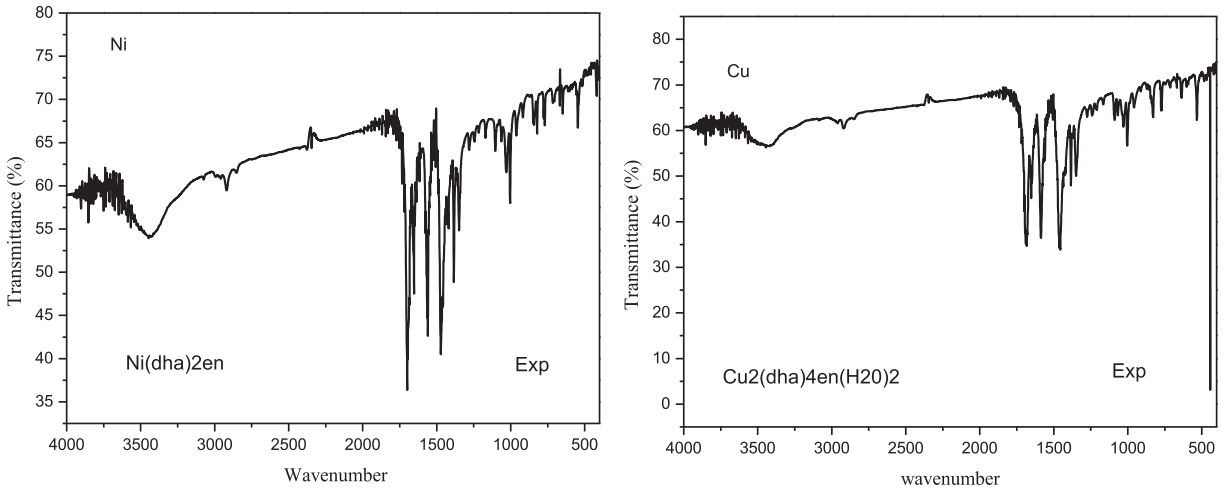

Fig. 1. Infrared spectrum of (a) [NiL] and (b) **[$Cu_2L_2H_2O$], H_2O**.

Table 1
Crystallographic data for [NiL] and **[$Cu_2L_2H_2O$], H_2O**.

Compound	[NiL]	**[$Cu_2L_2H_2O$], H_2O**
Molecular formula	$C_{18}H_{18}N_2NiO_6$	$C_{36}H_{40}Cu_2N_4O_{14}$
Molecular weight	417.05	879.80
Temperature (K)	293	293
Radiation	Mo Kα radiation(λ = 0.71073 Å)	Mo Kα (λ = 0.71073 Å)
Crystal system	Monoclinic	Triclinic
Crystal colour	Orange	Blue
Space group	$P2_1/c$	P-1
a(A°)	12.905 (5)	0.601(5)
b(A°)	13.575 (5)	12.928(5)
c(A°)	10.167 (5)	14.778(5)
Alpha°	90.000 (5)	70.230 (5)°
Beta°	104.374 (5)	88.950 (5)°
Gamma°	90.000 (5)	74.203 (5)°
Z	4	2
V/A^3	1725.4 (13)	1827.9 (13)
D_{calc}(g cm^{-3})	1.606	1.599
Crystal description	needle	needle
Absorption coefficient (mm^{-1})	1.16	1.24
F(000)	864	908
Reflections collected/ unique	12472/3543[R_{int} = 0.038]	20580/11511 [R_{int} = 0.049]
Range/indices (h,k,l)	−15, 16; −16, 13; −12, 12	−7, 15; −19, 19; −20, 20
$Teta_{limit}$	1.6–26.4	1.6–26.4
No.of observed data, I > 2σ(I)	2555	7849
No.of variables	252	519
No.of restraints	2	4
Goodness of fit on F^2	1.041	1.068
Largestdiff. Peak and hole (eA^{-3})	0.37 and −0.35	2.03 and −1.54
$R[F^2 > 2\sigma(F^2)]$	0.043	0.077
w$R(F^2)$	0.128	0.243
Maximum Δ/σ	<0.001	0.276

The distances between nitrogen and oxygen atoms and the metal center (Table 2) are similar to the values found in the [Cu(dha)$_2$en($H_2$0)] [41] and Cu^{II} (*N,N′*-bis(salicylaldehyde)-2,2′-biphenyldiimine [42]. The bond angles O2–Cu1–O1, N2–Cu1–N1, O22–Cu2–O11, N22–Cu2–N11 are 88.85°, 88.01°, 88.08° and 87.47° respectively. The O–Cu–N angles in the basal plane are of 176.97 and 170.67° for Cu1 and 177.30 and 177.46 for Cu2 showing a small distortion in the geometry.

In fact, the packing analysis in the unit cell shows that two molecules of the complex are not close one to another, and a dimeric structure (face to face) is formed considering the weak inter-dimer electrostatic Cu2–O6 (pyrone) (Fig. 4a,b). In the dimer, the Cu···Cu distances is of 6.069(3) Å, which is significantly long than those distances found in the bis(salicylaldehydato) Cu(II) complex (4.05 Å) [43,44]. Indeed this Cu···Cu distance is comparable to those distances found in many dinuclear Cu(II) oxygen bridged complexes [45–48]. A water molecule serves as a link between the two ligands via two hydrogen bonds.

3.4. Electrochemical studies

Curve A (Fig. 5) shows the cyclic voltammograms of [NiL] complex in DMSO solution in the potential ranges of +1.8 to −2.2 V. The cyclovoltammograms of the nickel complex display quasi-reversible reductive response (Ep_c at −1.46 V) during cathodic scan, attributed to the Ni^{II}/Ni^{I} couple. During the anodic potential scan, the complex shows an irreversible oxidative response at +1.39 V that may be assigned to the oxidation of the Schiff base.

As can be seen also, a well-defined redox peak with formal potential of −1.41 V versus SCE electrode was observed (Fig. 5B). These anodic and cathodic peaks are due to redox reaction of the Ni(II)/Ni(I) couple at the electrode surface. The potential was cycled between −0.7 and −1.8 V for the Ni(II)/Ni(I) redox system in DMSO solution and a large peak-to-peak separation (ΔE = 110 mV), indicating a quasi-reversible nature for the Ni^{II}/Ni^{I} reductive response. The electrochemical behavior and the data are in agreement with those reported for related complexes [49].

Fig. 6 shows the cyclic voltammograms of **[$Cu_2L_2H_2O$], H_2O** complex in DMSO solution in the potential ranges of +1.8–−2.2 V. The cyclovoltammogram of the copper complex display irreversible reductive responses (Ep_c at −0.95 and −1.55 V, respectively) during cathodic scan, attributed to the Cu^{II}/Cu^{I} couple. During the anodic potential scan, the complex shows an oxidative response at −0.10 V with very thin size (Fig. 6B) and high peak current and irreversible oxidative responses at +1.24 V (Fig. 6A). The response at −0.10 V is typical of the anodic stripping of copper. Therefore, it may be inferred that the Cu(II) complex undergo reduction to their

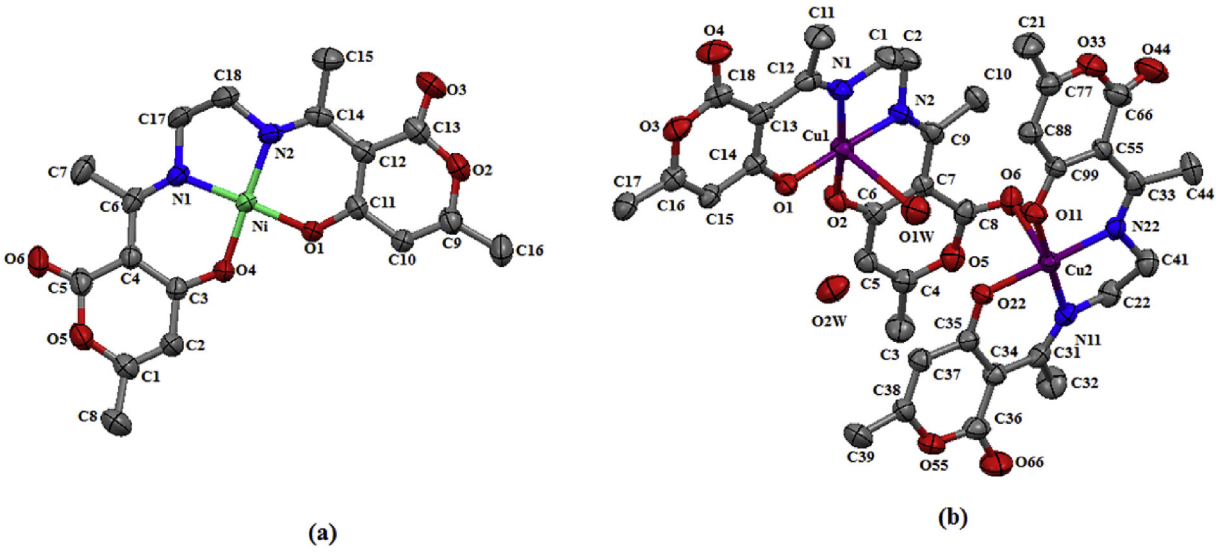

Fig. 2. The molecular structure of the [NiL] (a) and **[$Cu_2L_2H_2O$], H_2O** (b).

Table 2
Selected bond distances (Å) and angles (°) for [NiL] and **[$Cu_2L_2H_2O$], H_2O** complexes.

Bond lengths (Å)		Bond angles (°)	
[NiL]			
Ni–O1	1.832 (2)	O1–Ni–O4	84.90 (10)
Ni–O4	1.839 (2)	O1–Ni–N2	93.17 (11)
Ni–N1	1.854 (3)	O4–Ni–N1	92.64 (11)
Ni–N2	1.851 (3)	N2–Ni–N1	89.33 (12)
N1–C6	1.300 (5)	C3–O4–Ni	126.5 (2)
N1–C17	1.476 (4)	C11–O1–Ni	128.20 (2)
N2–C14	1.306 (4)	C6–N1–Ni	129.7 (2)
N2–C18	1.486 (4)	C17–N1–Ni	109.08 (2)
O1–C11	1.283 (4)	C14–N2–Ni	129.9 (2)
O4–C3	1.284 (4)	C18–N2–Ni	100.0 (2)
		O4– Ni– N2	177.54(12)
		O1– Ni– N1	176.99(12)
		C14– N2– C18	120.0(3)
		C6– N1– C17	120.4(3)
		N1– C17– C18	107.5(3)
		N2– C18– C17	107.7(3)
[$Cu_2L_2H_2O$], H_2O			
Cu1–O2	1.903(2)	O2–Cu1–O1	88.85(11)
Cu1–O1	1.914(3)	O1–Cu1–N1	91.83(12)
Cu1–N2	1.931(3)	O1–Cu1–N2	176.97(12)
Cu1–N1	1.936(3)	O2–Cu1–N1	170.68(13)
Cu1–O1w	2.705(3)	N2–Cu1–N1	88.01(13)
Cu2–O22	1.910(3)	O2–Cu1–N2	91.80(12)
Cu2–O11	1.910(2)	C9–N2–Cu1	128.4(2)
Cu2–N22	1.930(3)	C2– N2 Cu1	109.5(3)
Cu2–N11	1.948(3)	C14 –O1 Cu1	126.7(2)
Cu2–O5	2.699(3)	C6 –O2 –Cu1	124.2(2)
N22–C33	1.296(4)	C12 –N1– Cu1	129.5(3)
N22–C41	1.478(4)	C1– N1–Cu1	108.8(2)
N11–C31	1.293(5)	O22–Cu2–N22	177.30(11)
N11–C22	1.470(5)	O22–Cu2–O11	88.08(11)
C12–N1	1.300(5)	O11–Cu2–N22	92.63(11)
N2–C9	1.298(5)	O22–Cu2–N11	91.94(11)
N2–C2	1.468(4)	O11–Cu2–N11	177.48(12)
N1–C1	1.478(5)	N22–Cu2–N11	87.47(12)
O1–C14	1.280(4)	C99–O1–Cu2	125.7(2)
O2–C6	1.283(4)	C35– O22–Cu2	126.4(2)
O22–C35	1.274(4)	C33–N22 –Cu2	129.4(2)
O11–C99	1.279(4)	C41– N22– Cu2	109.8(2)
O6–C8	1.215(4)	C31– N11– Cu2	129.0(2)
		C22– N11– Cu2	108.2(2)

respective Cu(I) complex which subsequently undergo disproportionation to Cu^0 and Cu^{II}. The instability of the Cu(I) complex is in agreement with the literature [50]. The oxidative responses around 1.24 V may be due to the Cu^{II}/Cu^{III} couple.

4. Computational methods

The ground state optimizations of complexes [NiL] and **[$Cu_2L_2H_2O$], H_2O** have been carried out in the framework of DFT using the global hybrid B3LYP functional in combination with 6-311G (d,p) basis sets for C,N,O and H, and LANL2DZ pseudo potential and basis set [51] for Ni and Cu metals. In the following, Gen refers to Lanl2dz (for Cu, Ni) and 6-311G(d,p) (for N,O,H,C). Electronic excited states calculations have been performed in the framework of the time-dependent density functional theory (TDDFT) using B3LYP and the Gen basis set. Excited states and charge transfer character of electronic transitions were characterized by plotting the electron density and using the Natural transition orbitals (NTOs) [52,53].

4.1. Optimized structure

The optimization structures and the geometrical parameters such as bond lengths, and bond angles are given in Table 3. Concerning the complex of [NiL] the metal-ligand bond distances are slightly longer than the experimental values within 0.014–0.034 Å range. The calculated bond distances of Ni–O and Ni–N are 1.853 and 1.880 Å respectively compared to the experimental values of 1.832–1.839 Å and 1.854 Å respectively. The binuclear complex of **[$Cu_2L_2H_2O$], H_2O** is characterized by its asymmetric unit containing one complex molecule and one water molecule. The structure reveals that the two Cu(II) center is "4 + 1" coordinated, exhibiting a distorted tetragonal pyramid geometry in which the basal plane is occupied by two oxygen atoms from the phenolates and two nitrogen atoms from the imine groups of the ligand, the axial position of Cu1 is occupied by O1w atom of water molecular and one pyrone oxygen from another moiety, in axial positions from Cu2. The **[$Cu_2L_2H_2O$], H_2O** complex has a square-planar geometry connected via two phenolic oxygen O_2 and O_5 and imine nitrogen N_8 and N_{11}. For [NiL] the calculated values are in good agreement with the experiments, since all differences between the theoretical and experimental bond lengths are in 0.034–0.08 Å. The calculated ligand-metal-ligand bond angles for the two complexes are almost similar to the experimental values with slight deviations within for 0.09–1.85°of the complex [NiL] and 0.41°–5.28° for the complex [$Cu_2L_2H_2O$], H_2O.

4.2. Harmonic vibrational frequencies

Experimental and calculated IR spectra of [NiL] and **[$Cu_2L_2H_2O$], H_2O** are shown in Fig. 7a,b. A rigorous analysis for modes of vibration with B3LYP level is mentioned in Table 4. The calculated values are globally in good agreement with the experimental data. The experimental FTIR band at 3435 cm^{-1} assigned to intermolecular hydrogen bonded ν(OH) for **[$Cu_2L_2H_2O$], H_2O** is calculated at 3432 cm^{-1} at B3LYP/Gen level. The lactone ν(C–O) stretch vibration

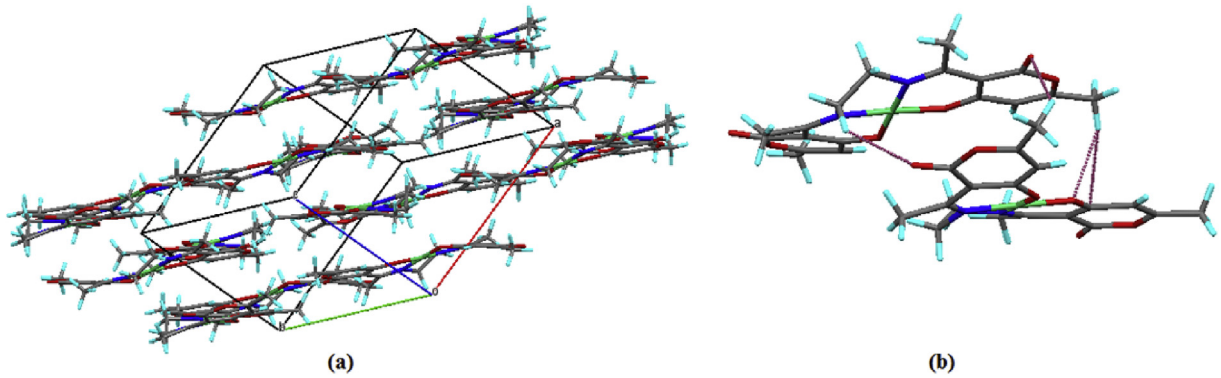

Fig. 3. Cell packing (a) and hydrogen bonding (b) for [NiL].

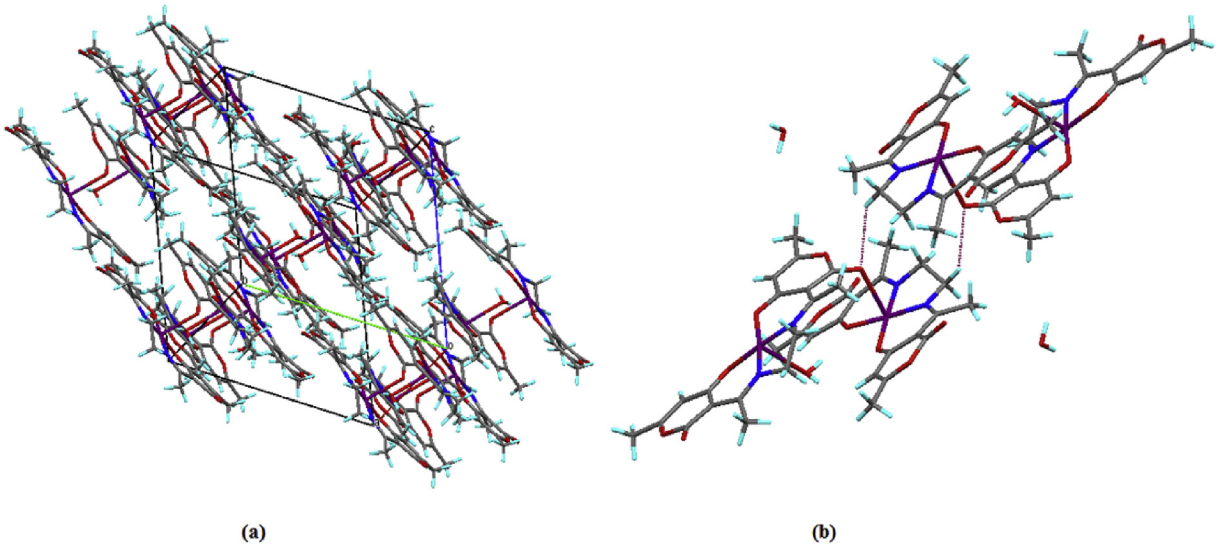

Fig. 4. Cell packing (a) and hydrogen bonding (b) for **[$Cu_2L_2H_2O$], H_2O**.

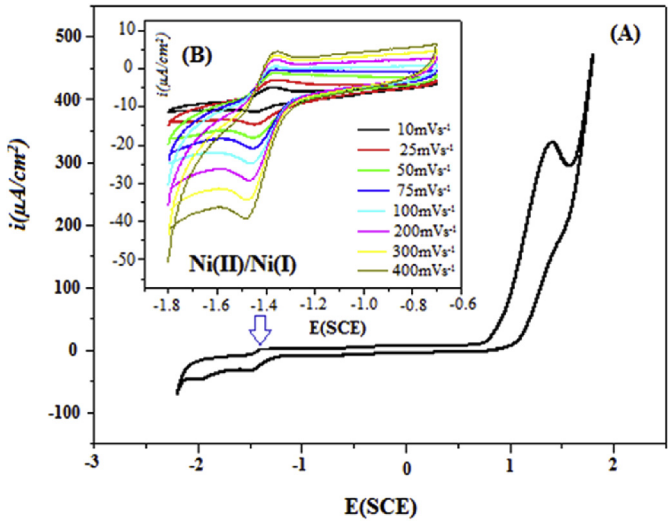

Fig. 5. Cyclic voltammogram of [NiL] in the range +1.8 to −2.2 V (**A**); and in the range −0.7 to −1.8 at different scan rates for (**B**).

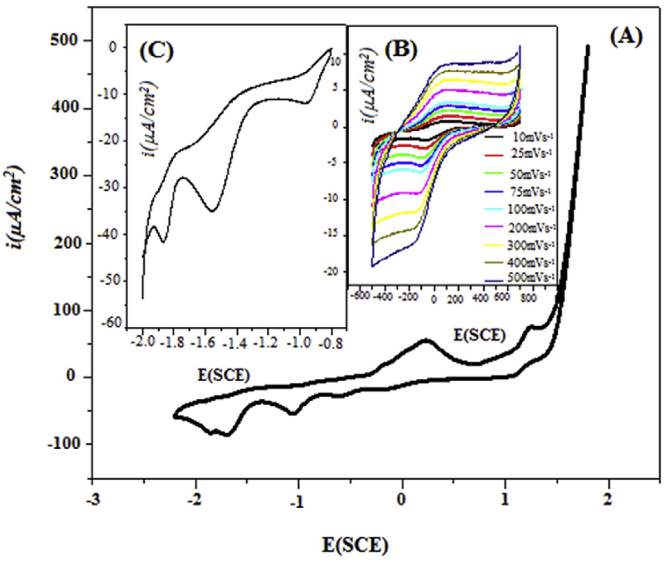

Fig. 6. Cyclic voltammogram of [$Cu_2L_2H_2O$], H_2O in the range +1.8−−2.2 V (A); −0.6−−2.0 (C) and +0.5−−0.5 at different scan rates for (B).

appears in the region 1226 cm^{-1} in experiment, while it is calculated at 1256 cm^{-1} for complex [NiL] and 1215 cm^{-1} for **[$Cu_2L_2H_2O$], H_2O**. The frequency for carbonyl ν(C═O) has been calculated at 1701 cm^{-1} for the complex of Ni and 1694 cm^{-1} for complex of Cu, in excellent agreement with experimental data of 1700 cm^{-1} and 1691 cm^{-1} respectively. The experimental data of the ν(C═N) stretching vibration is 1378 cm^{-1} for the complex of Cu metal and 1560 cm^{-1} for the complex of Ni metal, these bands have been calculated at 1385 cm^{-1} and 1597 cm^{-1}. The lower frequency region above 594 cm^{-1} for [NiL] and 567 cm^{-1} for **[$Cu_2L_2H_2O$], H_2O** is the characteristic region for identification of ν(M—O) and ν(M—N) while these bands were computed at 591 cm^{-1} for complex of Ni and 577 cm^{-1} for complex of Cu respectively.

4.3. Uv–vis absorption

Absorption wavelengths in gas phase have been simulated at TDDFT/B3LYP level. Main electronic transitions can be found in Table 5, while the excited states and charge transfer character of electronic transitions are characterized by plotting the Natural Transition Orbitals for main states in Fig. 8.

For the complex [NiL], three absorption features have been calculated in the visible region, in good agreement with the well resolved experimental data. The NTO analysis shows that this transition is an absorption band at the 350 nm that originates mainly in the HOMO → LUMO electronic transition, a second band calculated at 310 nm with a main contribution from HOMO-1 → LUMO + 2 transition which is primarily π → d, a third transition is calculated at 278 nm due to the transfer charge from n→π and mainly originates from the HOMO-3 → LUMO. For the [$Cu_2L_2H_2O$], H_2O the lowest energy absorption is calculated at 562 nm and originates from the HOMO → LUMO + 1 transition associated to a charge transfer (CT) from d_{Cu1} orbitals to ligand and a Cu2 transfer MLCT, while the second transition calculated at 374 nm is attributed to d_{Cu1} to π ligand charge transfer. The

Table 3
Selected bond lengths (Å) and angles (°) for **[$Cu_2L_2H_2O$], H_2O** and [NiL].

	B3LYP/Gen	Exp
[NiL]		
Bond length (Å)		
Ni–O2	1.853	1.832
Ni–O5	1.853	1.839
Ni–N11	1.888	1.854
Ni–O2	1.853	1.832
Angles (°)		
O5–Ni– N11	92.02	93.17
O2– Ni –N8	92.02	92.64
O5– Ni –O2	86.75	84.90
N8– Ni –N11	89.24	89.33
[$Cu_2L_2H_2O$], H2O		
Bond length(Å)		
Cu1– O7	1.990	1.914
Cu1–O5	1.979	1.903
Cu1–N17	1.994	1.936
Cu1–N15	2.011	1.931
Cu2– O8	1.987	1.910
Cu2–O10	1.975	1.910
Cu2–N22	1.982	1.948
Cu2–N24	1.988	1.930
Angles (°)		
O15–Cu1–O17	87.60	88.01
N15–Cu1–O5	89.98	88.95
O5–Cu1–N17	94.10	88.85
O7–Cu1–N17	88.70	91.80
O7–Cu1–N15	174.94	177.3
N17–Cu1–O5	173.47	170.68
O24–Cu2–N22	87.12	87.47
N22–Cu2–O8	89.98	88.95
O10–Cu2–N24	88.08	91.94
O10–Cu2–N22	91.058	88.08
N24–Cu2–O8	173.48	177.48

absorption band at 312 nm mainly involved the HOMO-3→LUMO+2 transition it can be characterized by n-π^* as shown in Fig. 8. Finally, the absorption at 260 nm presents an obvious $\pi \rightarrow d$ character and mainly originates from HOMO-1 → LUMO + 5.

Table 4
Comparison of the experimental and calculated vibrational frequencies (cm^{-1}) for [NiL] and **[$Cu_2L_2H_2O$], H_2O** complexes.

Assignement (cm^{-1})	**[NiL]**		**[$Cu_2L_2H_2O$], H_2O**	
	B3LYP	Exp	B3LYP	Exp
ν (O_w–H) (stretching)	–	–	3512	3435
ν (C=O) (stretching)	1701	1700	1694	1691
ν (C=N) (stretching)	1597	1560	1385	1378
ν(C–O) (stretching)	1256	1226	1215	1226
ν(M–O) (stretching)	690	694	639	625
ν(M–N) (stretching)	591	594	577	567

Table 5
Experimental λ_{exp}(nm) and calculated λ_{Th}(nm) wavelengths and *f* oscillator strength for [NiL] and **[$Cu_2L_2H_2O$], H_2O**.

	[NiL]				**[$Cu_2L_2H_2O$], H_2O**			
	B3LYP				B3LYP			
	λ_{Th}	*f*	λ_{exp}	Major contribution	λ_{Th}	*f*	λ_{exp}	Major contribution
Band I	278	0.014	281	H – 3 → L	260	0.0015	260	H – 1 → L + 5
Band II	310	0.001	310	H – 1 → L + 2	312	0.033	312	H – 3 → L + 2
Band III	350	0.046	370	H → L	374	0.0012	374	H → L + 4
Band IV	–	–	–	–	562	0.0003	568	H → L + 1

5. Conclusion

In this paper, we have described the [NiL] and [$Cu_2L_2H_2O$], H_2O complexes. The metal center has square-planar coordination geometry for the complex of Ni metal and square pyramidal coordination geometry for the complex of Cu metal. The redox behavior was investigated by cyclic voltammetry. The metal complexes show both anodic and cathodic peaks which are due to redox reaction of the Ni^{II}/Ni^{I}, Cu^{II}/Cu^{I} and Cu^{0}/Cu^{II} at the electrode surface for NiL and [$Cu_2L_2H_2O$], H_2O respectively. The theoretical study for both

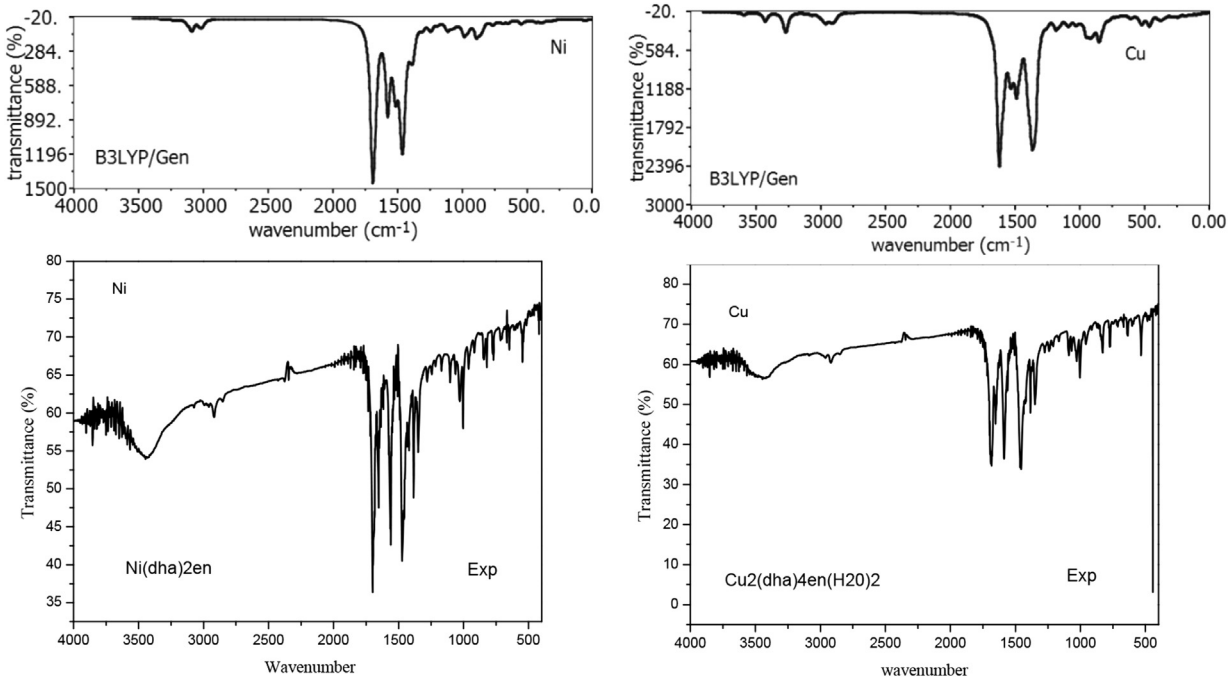

Fig. 7. Simulated versus experimental infrared spectra of [NiL]and **[$Cu_2L_2H_2O$], H_2O**.

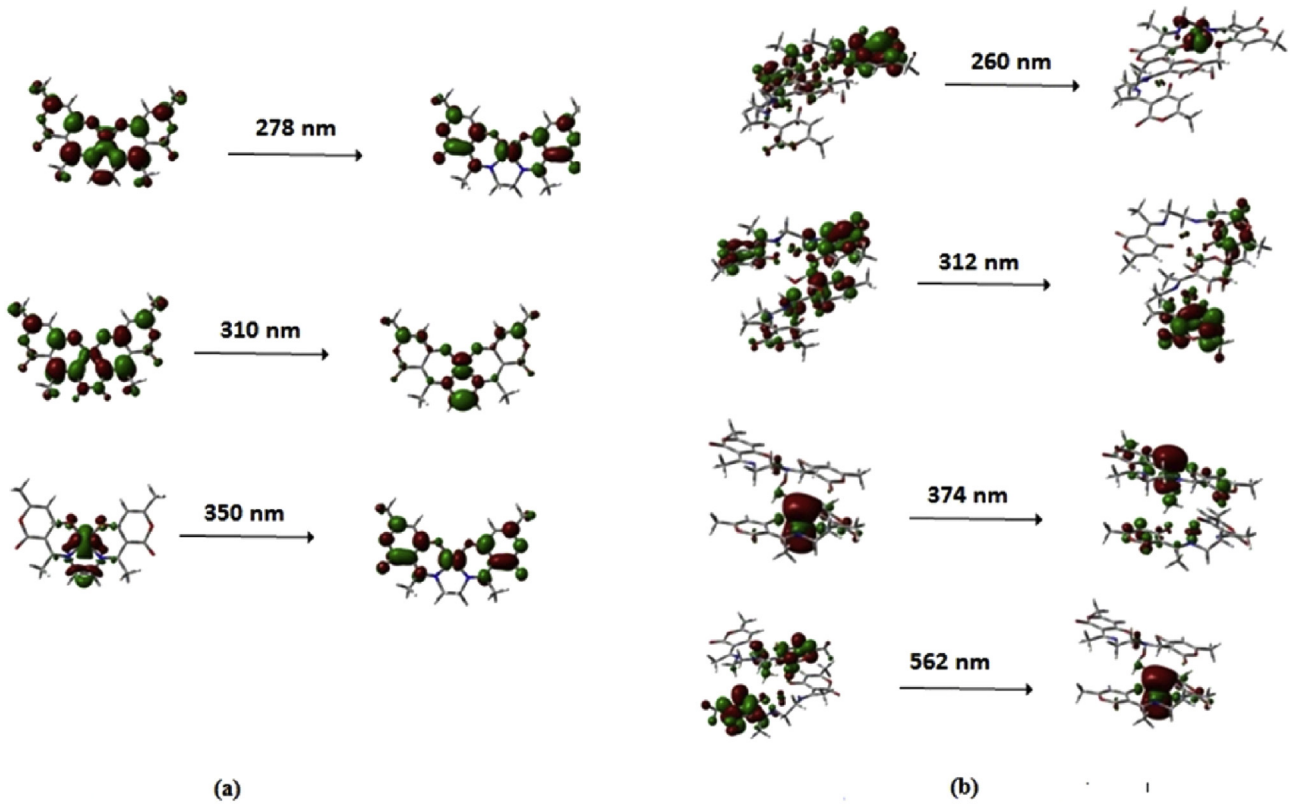

Fig. 8. Contour plots of the natural transition orbitals (NTOs) for both [NiL] **(a)** and **[$Cu_2L_2H_2O$], H_2O (b)**.

complexes on structural parameters, IR spectra, and UV–vis absorption gives values in excellent agreement with the experimental data.

Acknowledgement

We are grateful to MESRS and DGRSDT (Algeria) for financial support. We gratefully acknowledge support from the PSMN (Pôle Scientifique de Modélisation Numérique) computing center at Lyon, France.

References

[1] I. Sylvestre, J. Wolowska, E.J.L. McInnes, C.A. Kilner, M.A. Halcrow, Inorg. Chem. Acta 358 (2005) 1337–1341.
[2] M. Thirumavalavan, P. Akilan, P. Amudha, M. Kandaswamy, Polyhedron 23 (2004) 519–527.
[3] N. Mondal, S. Mitra, V. Gramlich, S.O. Ghodsi, K.M.A. Malik, Polyhedron 20 (2001) 135–141.
[4] M. Amirnasr, K.J. Schenk, S. Meghdadi, M. Morshedi, Polyhedron 25 (2006) 671–677.
[5] A. Bouchama, A. Bendaàs, C. Chiter, A. Beghidja, A. Djedouani, Acta Cryst. E 63 (2006) m2397.
[6] A. Djedouani, A. Bendaàs, S. Bouacida, A. Beghidja, T. Douadi, Acta Cryst. E 62 (2006) m133–m135.
[7] M. Cindric, V. Vrdoljak, T.K. Novak, M. Curic, A. Brbot-Saranovic, B. Kamenar, J. Mol. Struct. 701 (2004) 111–118.
[8] M.Z. Chalaca, J.D. Figueroa-Villar, J.A. Ellena, E.E. Castellano, Inorg. Chim. Acta 328 (2002) 45–52.
[9] S.M. Jadhav, V.A. Shelke, S.G. Shankarwar, A.S. Munde, T.K. Chondhekar, J. Saudi Chem. Soc. 18 (2014) 27–34.
[10] S.A. Munde, N.A. Jagdale, M.S. Jadhav, K.T. Chondhekar, J. Serb. Chem. Soc. 75 (2010) 349–359.
[11] R.I. Kureshy, N.H. Khan, S.H.R. Abdi, P. Iyer, S.T. Patel, Polyhedron 18 (1999) 1773–1777.
[12] R.I. Kureshy, N.H. Khan, S.H.R. Abdi, P. Iyer, J. Mol. Catal. 124 (1997) 91–97.
[13] P.V. Rao, A.V. Narasaiah, Indian J. Chem. A 42 (2003) 1896–1899.
[14] D.T. Puerta, S.M. Cohen, Inorg. Chem. 42 (2003) 3423–3430.
[15] G. Battaini, E. Monzani, L. Casella, L. Santagostini, R. Pagliarin, J. Biol. Inorg. Chem. 5 (2000) 262–268.
[16] S. Thaisrivongs, D.L. Romero, R.A. Tommasi, M.N. Janakiraman, J.W. Strohbach, S.R. Turner, C. Biles, R.R. Morge, P.D. Johnson, P.A. Aristoff, P.K. Tomich, J.C. Lynn, M.M. Horng, K.T. Chong, R.R.W.J. Howe, B.C. Finzel, K.D. Watenpaugh, J. Med. Chem. 32 (1996) 4630–4642.
[17] T.I. Kashar, A.H. El-Sehli, J. Chem. Pharm. Res. 5 (2013) 474–483.
[18] S. Thaisrivongs, D.L. Romero, R.A. Tommasi, M.N. Janakirman, J.W. Strohbach, S.R. Turner, C. Biles, R.R. Morge, P.D. Johnson, P.A. Aristoff, P.K. Tomich, J.C. Lymn, M.M. Horng, K.T. Chong, R.R. Hinshaw, W.J. Howe, B.C. Finzel, K.D. Watenpaugh, J. Med. Chem. 39 (1996) 4630–4642.
[19] P.A. Wolf, W.M. Westveer, Arch. Biochem. 28 (1950) 201–206.
[20] S.G. Shirodkar, P.S. Mane, T.K. Chondhekar, Indian, J. Chem. 40 (2001) 1114–1117.
[21] V.A. Shelke, S.M. Jadhav, V.R. Patharkar, S.G. Shankarwar, A.S. Munde, T.K. Chondhekar, J. Saudi. Chem. Soc. 5 (2012) 501–507.
[22] M86-E01078 APEX2 User Manual, Bruker AXS Inc., Madison, USA, 2006.
[23] G.M. Sheldrick, SHELXS-97 program for crystal structure determination, Acta Crystallogr. A46 (1990) 467–473.
[24] G. Sheldrick, SHELXL-97, Universität Göttingen, Göttingen, Germany, 1999.
[25] M.J. Frisch, G.W. Trucks, H.B. Schlegel, G.E. Scuseria, M.A.n Robb, J.R. Cheeseman, G. Scalmani, V. Barone, B. Mennucci, G.A. Petersson, H. Nakatsuji, M. Caricato, X. Li, H.P. Hratchian, A.F. Izmaylov, J. Bloino, G. Zheng, J.L. Sonnenberg, M. Hada, M. Ehara, K. Toyota, R. Fukuda, J. Hasegawa, M. Ishida, T. Nakajima, Y. Honda, O. Kitao, H. Nakai, T. Vreven, J.A. Montgomery, Jr, J.E. Peralta, F. Ogliaro, M. Bearpark, J.J. Heyd, E. Brothers, K.N. Kudin, V.N. Staroverov, R. Kobayashi, J. Normand, K. Raghavachari, A. Rendell, J.C. Burant, S.S. Iyengar, J. Tomasi, M. Cossi, N. Rega, J.M. Millam, M. Klene, J.E. Knox, J.B. Cross, V. Bakken, C. Adamo, J. Jaramillo, R. Gomperts, R.E. Stratmann, O. Yazyev, A.J. Austin, R. Cammi, C. Pomelli, J.W. Ochterski, R.L. Martin, K. Morokuma, V.G. Zakrzewski, G.A. Voth, P. Salvador, J.J. Dannenberg, S. Dapprich, A.D. Daniels, O. Farkas, J.B. Foresman, J.V. Ortiz, J. Cioslowski, D.J. Fox, Gaussian Inc, Wallingford, CT, (2009).
[26] W. Kohn, L.J. Sham, Phys. Rev. 140 (1965) A1133–A1138.
[27] A.D. Becke, J. Chem. Phys. 98 (1993) 5648–5652.
[28] C. Lee, W. Yang, R.G. Parr, Phys. Rev. B 37 (1998) 785–789.
[29] T. Sau-fun, A. Kok-Peng, Transit. Met. 13 (1988) 64–68.
[30] N. Batra, J. Devi, J. Chem. Pharm. Res. 2 (2015) 183–189.
[31] N.S.K. Agrawal, D.R. Tuflani, R. Gupta, S.K. Hajela, Inorg. Chim. Acta 129 (1987) 257–259.
[32] O. Carugo, C.B. Castellani, M. Rizzi, Polyhedron 9 (1990) 2061–2069.
[33] Tahani I. Kashar, Amal H. El-Sehli, J. Chem. Pharm. Res. 5 (11) (2013) 474–483.

[34] S.M. Jadhav, V.A. Shelke, S.G. Shankarwar, A.S. Munde, T.K. Chondhekar, J. Saudi Chem. Soc. 18 (2014) 27–34.
[35] D.M. Fouad, A. Bayoumi, M.A. El-Gahami, S.A. Ibrahim, A.M. Hammam, Nat. Sci. 2 (2010) 817–827.
[36] A. Golco, M. Tumer, H. Demirelli, R.A. Wheatly, Inorg. Chim. Acta 358 (2005) 1785–1797.
[37] M. Tumer, Synth. React. Inorg. Met. Chem. 30 (2000) 1139–1158.
[38] J. Losada, I.D. Peso, L. Beyer, Synthesis, electrochemical properties and electro-oxidative polymerization of copper(II) and nickel(II) complexes with N-benzoylthiourea ligands containing pyrrole groups, Transit. Met. Chem. 25 (2000) 112–117.
[39] O. Diouf, Diariatou Gningue Sall, Mohamed Lamine Gaye, Abdou Salam Sall, C. R. Chim. 10 (2007) 473–481.
[40] S.M. Emam, A.S. El-Tabl, H.M. Ahmed, E.A. Emad. J. Arab. http://dx.doi.org/10.1016/j.arabjc.2014.05.019.
[41] L.M. Shkolnikova, E.M. Yumal, E.A. Shugam, V.A. Voblikova, Zh. Strukt. Khim. 11 (1970) 886–890.
[42] L. Ting-Fong, T. Sau-fun, A. Kok-Peng, C.W.M. Thomas, Transit. Met. Chem. 10 (1985) 375–379.
[43] D. Hall, A.J. McKinnon, T.N. Waters, J. Chem. Soc. (1965) 425.
[44] P.D.W. Boyd, A.D. Toy, T.D. Smith, J.R. Pilbrow, J. Chem. Soc. (1973) 1549–1563.
[45] W.B. Tolman, Acc. Chem. Res. 30 (1997) 227–237.
[46] A. Neves, L.M. Rossi, A.J. Bortoluzzi, B. Szpoganicz, C. Wiezbicki, E. Schwingel, W. Haase, S. Ostrovsky, Inorg. Chem. 41 (2002) 1788–1794.
[47] A. Neves, L.M. Rossi, I. Vencato, V. Drago, W. Haase, R. Werner, Inorg. Chim. Acta 281 (1998) 111–115.
[48] R.A. Peralta, A. Neves, A.J. Bortoluzzi, A. dos Anjos, F.R. Xavier, B. Szpoganicz, H. Terenzi, M.C.B. de Oliveira, E. Castellano, G.R. Friedermann, A.S. Mangrich, M.A. Novak, J. Inorg. Biochem. 100 (2006) 992–1004.
[49] P. Mukherjee, M.G.B. Drew, A. Ghosh, Eur. J. Inorg. Chem. (2008) 3372.
[50] B. Sarkar, S. Konar, C.J. Gomez-Garcia, A. Ghosh, Inorg. Chem. 47 (2008) 11611.
[51] P.J. Hay, W.R. Wadt, J. Chem. Phys. 82 (1985) 299.
[52] R.L. Martin, J. Chem. Phys. 118 (2003) 4775–4777.
[53] L.E. Roy, G. Scalmani, R. Kobayashi, E.R. Batista, Dalton Trans. (2009) 6719–6721.